(1)

SBIR Phase I Final Report

a. Contractor: Conductus, 969 West Maude Avenue, Sunnyvale, CA 94086

b. SDIO Contract number: DASG60-93-C-0118

c. Effective Date of Contract: 04 June 93

d. Expiration Date of Contract (with extension): 28 February 94

e. Reporting Period: 04 June 93 - 28 February 94.
Report Submitted: 19 May, 1994

f. Principal Investigator: J. Kelly Truman, Ph.D.
408-524-9819

h. Title: HTS SNS Devices on Large-Area Substrates by Single-Source MOCVD

Sponsored by

SDIO Innovative Science and Technology Office

Managed by

U.S. Army Strategic Defense Command

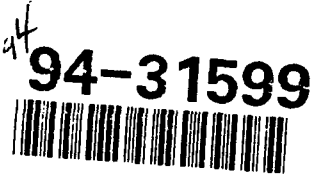

421 894

94

CONDUCTUS, INC. CONTRACT DASG60-93-C-0118

SECURITY CLASSIFICATION OF THIS PAGE

REPORT DOCUMENTATION PAGE

Form Approved OMB No. 0704-0188

1a. REPORT SECURITY CLASSIFICATION: unclassified	1b. RESTRICTIVE MARKINGS: none
2a. SECURITY CLASSIFICATION AUTHORITY: na	3. DISTRIBUTION/AVAILABILITY OF REPORT: unlimited
2b. DECLASSIFICATION/DOWNGRADING SCHEDULE: na	
4. PERFORMING ORGANIZATION REPORT NUMBER(S): na	5. MONITORING ORGANIZATION REPORT NUMBER(S): na
6a. NAME OF PERFORMING ORGANIZATION: Conductus, Inc; 6b. OFFICE SYMBOL (If applicable):	7a. NAME OF MONITORING ORGANIZATION: U.S. Army Space and Strategic Defense Command
6c. ADDRESS (City, State, and ZIP Code): 969 West Maude Ave, Sunnyvale, CA 94086	7b. ADDRESS (City, State, and ZIP Code): Contr. & Acq Mgt Ofc, CSSD-CM-TC, PO Box 1500, Huntsville, AL 35807-3801
8a. NAME OF FUNDING/SPONSORING ORGANIZATION: SDIO Innovative Science & Tech Office; 8b. OFFICE SYMBOL (If applicable):	9. PROCUREMENT INSTRUMENT IDENTIFICATION NUMBER: Contract # DASG60-93-C-0118
8c. ADDRESS (City, State, and ZIP Code): Pentagon, Washington, DC 20301-7100	10. SOURCE OF FUNDING NUMBERS: PROGRAM ELEMENT NO. / PROJECT NO. / TASK NO. / WORK UNIT ACCESSION NO.

11. TITLE (Include Security Classification)

Development of HTS SNS Devices on Large Area Substrates by Single Source MOCVD

12. PERSONAL AUTHOR(S) Truman, J. Kelly

13a. TYPE OF REPORT	13b. TIME COVERED	14. DATE OF REPORT (Year, Month, Day)	15. PAGE COUNT
final	FROM 930694 TO 940228	1994, May, 18	16

16. SUPPLEMENTARY NOTATION

17. COSATI CODES			18. SUBJECT TERMS (Continue on reverse if necessary and identify by block number)
FIELD	GROUP	SUB-GROUP	

19. ABSTRACT (Continue on reverse if necessary and identify by block number)

A novel, single-source metalorganic chemical vapor deposition (SSMOCVD) technique has shown exceptional promise for the growth of epitaxial oxide films and multilayers on large area substrates, as needed for the commercial-scale production of high temperature superconductor devices and circuits. In this contract the SSMOCVD technique was applied to growth of $YBa_2Cu_3O_{7-x}$ and $CaRuO_3$ films and multilayers for the fabrication of superconductor-normal-superconductor Josephson junctions. A process was developed for the growth of epitaxial $CaRuO_3$ films by SSMOCVD, which was the first reported growth of $CaRuO_3$ by MOCVD. Also, a process was developed for the *in situ* growth of epitaxial $YBa_2Cu_3O_{7-x}/CaRuO_3$ multilayers by SSMOCVD. Finally, epitaxial SNS edge junctions were fabricated and tested which used a top $YBCO/CaRuO_3$ bilayer grown *in situ* by SSMOCVD and a base $SrTiO_3/YBa_2Cu_3O_{7-x}$ bilayer grown *in situ* by pulsed laser ablation.

20. DISTRIBUTION/AVAILABILITY OF ABSTRACT	21. ABSTRACT SECURITY CLASSIFICATION
☑ UNCLASSIFIED/UNLIMITED ☐ SAME AS RPT. ☐ DTIC USERS	unclassified
22a. NAME OF RESPONSIBLE INDIVIDUAL: J. Kelly Truman, Ph.D.	22b. TELEPHONE (Include Area Code): 408-524-9819 / 22c. OFFICE SYMBOL

DD Form 1473, JUN 86 Previous editions are obsolete. SECURITY CLASSIFICATION OF THIS PAGE

A. Technical Problems

To meet the yield and volume requirements for the commercialization of high temperature superconductor (HTS) devices and circuits, a thin film deposition process is required which can produce a large number of devices with uniform properties across substrates as large as four inches in diameter. A key device technology required for a variety of Conductus' commercial HTS products is the superconducting-normal-superconducting (SNS) Josephson junction. A $YBa_2Cu_3O_{7-x}$ (YBCO) based SNS junction has been developed at Conductus which uses $CaRuO_3$ as the epitaxial normal barrier layer in the edge junction geometry, a schematic of which is shown in Figure 1 [1].

The performance of SNS edge junctions based on YBCO and $CaRuO_3$ is very promising for application to sensors as well as circuit elements in very high performance signal processing circuits such as shift registers, analog-to-digital converters, high-speed counters, and phase shifters. The critical current, specific normal state resistance, and noise properties of these junctions are superior to grain-boundary-based junctions. Since the critical current can be controlled by the thickness of the normal barrier material, which is on the order of hundreds of angstroms, the fabrication of SNS devices offers promise for large-scale production since this thickness can be controlled rather well. Further, this is far easier than controlling the thickness of the insulating barrier in a superconductor-insulator-superconductor tunnel junction, which is on the order of tens of angstroms. This fabrication control is the fundamental reason why one might believe that SNS junctions should be inherently controllable devices and provide the basis for a high temperature superconductor integrated circuit technology which can be aggressively pursued for commercial-scale production.

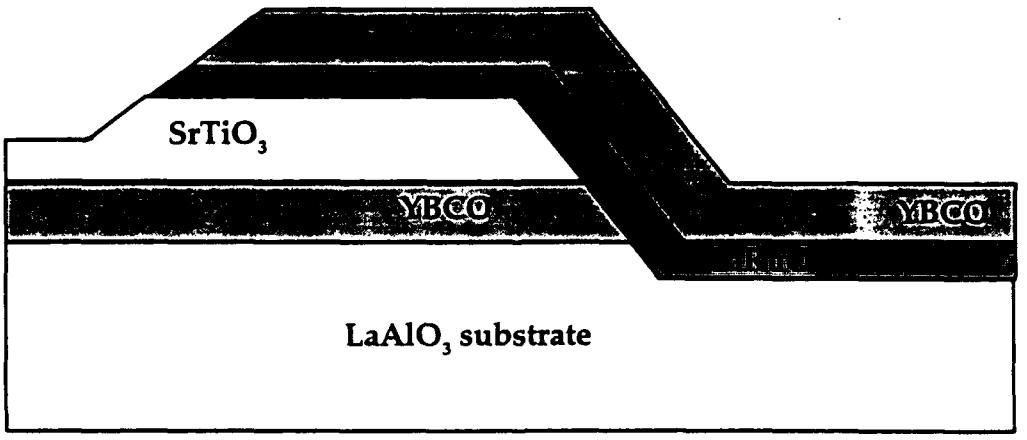

Figure 1. Schematic illustration of structure of Conductus' YBCO/$CaRuO_3$/YBCO SNS edge junction. The thickness of the YBCO and $SrTiO_3$ layers is ≅ 2000 Å, while that of the $CaRuO_3$ N layer is ≅ 100 Å.

Although the pulsed laser deposition technique currently used at Conductus for the fabrication of SNS junctions produces excellent results, it is presently limited in its capability to uniformly coat substrates larger than 1 cm^2. Thus only one or a few SNS devices can be produced per run. On the other hand, MOCVD provides inherent ease of scale-up to large area, short cycle times and high sample throughput, as required for a commercial thin film deposition technology. However, the development of MOCVD for YBCO films has been hampered by the difficulty of reproducibly transporting the metalorganic precursors to the substrate [2,3]. Standard delivery systems require control of the temperature and flow rate for each precursor. The metalorganic precursors used for MOCVD of YBCO, particularly that for Ba, exhibit a decreasing volatility with time when held at the required sublimation temperatures, making control of the film stoichiometry difficult [2,3].

The single-source MOCVD (SSMOCVD) technique, developed at Hewlett-Packard (HP) Laboratories and transferred to Conductus, effectively eliminates problems with the instability of the Ba precursor which has hampered the growth of YBCO by conventional MOCVD. A schematic of the SSMOCVD reactor is shown in Figure 2. Steady-state vaporization of the mixed powdered precursors occurs within a sharp temperature gradient in the vaporizer, such that a continuous source of fresh precursors are introduced into the vaporizer. Thus, the precursors are heated to the vaporization temperature for a short enough time to prevent significant decomposition. The SSMOCVD technique has been used to reproducibly grow high-quality epitaxial oxide thin films, including YBCO, and bilayers on a variety of substrates [4,5,6]. A

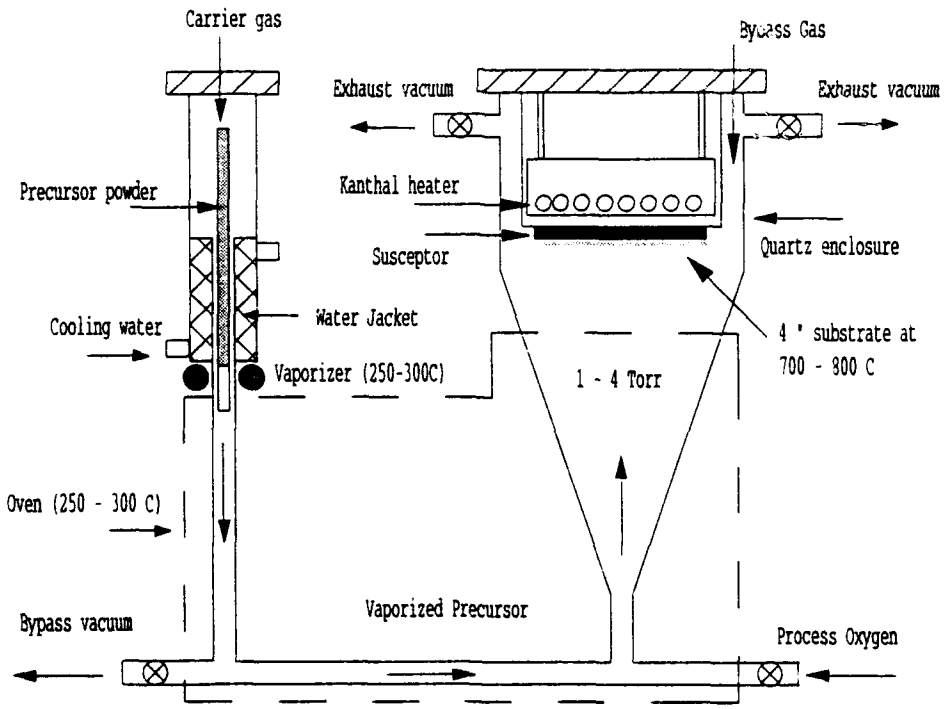

Figure 2. Schematic illustration of single source MOCVD technique for the epitaxial growth of oxide films.

simple process for the growth of high quality, epitaxial YBCO films on substrates from 1 cm^2 to 2 inches in diameter had been established prior to this contract at Hewlett-Packard (HP) for the SSMOCVD technique, and a process for 4-inch substrates was demonstrated. Thus SSMOCVD showed exceptional promise for the growth of YBCO, other oxide films, and multilayers on large area substrates, as needed for the commercial-scale production of high temperature superconductor devices and circuits.

B. Task Objectives

In this Phase I effort , the novel SSMOCVD technique was to be applied to the fabrication of HTS devices employing YBCO/$CaRuO_3$/YBCO SNS junctions. The growth of epitaxial $CaRuO_3$ films by single-source MOCVD had not yet been reported prior to the start of the contract, nor had a suitable solid metalorganic Ru precursor been identified. Further, the growth of HTS epitaxial multilayers (more than one HTS layer and one or more other epitaxial oxide layers) by MOCVD had not been previously reported. In particular. the fabrication of HTS SNS junctions by MOCVD had not been demonstrated. Thus, the technical objectives of this program were to:

1. evaluate candidate precursors for and develop the growth of $CaRuO_3$ by single-source MOCVD, for use as the barrier material in SNS junctions ,
2. fabricate $CaRuO_3$/YBCO bi-layers by SSMOCVD on 1 cm^2 and 2 inch diameter substrates, using the selected precursors for $CaRuO_3$, and test the properties of the bi-layer across the substrate,
3. fabricate edge junctions, as illustrated in Figure 1, on 1 cm^2 and 2 inch diameter substrates by single-source MOCVD and test the uniformity of critical current and resistance in the junctions across the substrate, and
4. demonstrate a functioning superconducting quantum interference device (SQUID) using $CaRuO_3$-based SNS junctions fabricated by single-source MOCVD.

C. General Methodology

All SSMOCVD film growth was performed using the general procedure that follows. Beta-diketonate powdered solid precursors were mixed and packed together in the desired ratios into a slotted quartz tube. The beta-diketonate powders which were used are summarized in Table 1. The growth of YBCO/$CaRuO_3$ bilayers and multilayer structures was accomplished by alternating the powdered precursor mixtures in the slotted tube. A spacer of quartz wool was placed between each powder mixture to ensure interface abruptness. The slotted tube was loaded into the reactor, which was evacuated by a mechanical pump to less than 100 mTorr. The Ar carrier gas rate was established. Concomitantly, the vaporizer and substrate temperature were stabilized at the typical desired values of 275 - 300 °C and 700 - 800 °C, respectively. The slotted tube was then slowly moved through an abrupt temperature gradient in the vaporizer, which used quartz lamps to heat the powder from room temperature to 275 - 300 °C in a space of less than 1 cm. The vaporized precursors were transported to the

Table 1. Summary of beta-diketonate metalorganic precursors used for SSMOCVD growth of YBCO and $CaRuO_3$

Precursor	Formula	Melting Point, C	Vendor
Y-TMHD	$Y(C_{11}H_{19}O_2)_3$	163 - 167	Strem Chemical
Ba-TMHD	$Ba(C_{11}H_{19}O_2)_2 \cdot xH_2O$	195 - 200	Strem Chemical
Cu-TMHD	$Cu(C_{11}H_{19}O_2)_2$	198	Strem Chemical
Ca-TMHD	$Ca(C_{11}H_{19}O_2)_2$	202 - 206	Strem Chemical
Ru-TMHD	$Ru(C_{11}H_{19}O_2)_3$	200 - 203	Strem Chemical

substrate by an Ar carrier gas. Oxygen was mixed with the vapor and carrier gas to permit *in situ* growth of epitaxial oxides on the heated substrate. The total pressure in the reactor was 0.75 - 4 Torr. The film growth rate was controlled by a combination of the rate at which the slotted tube is passed through the vaporizer, the carrier gas rate, and the total pressure. The film composition was effected by the precursor powder composition, and the vaporizer temperature, and the oxygen partial pressure. Typically, all growth parameters were held constant and the film composition was adjusted by changing the precursor powder composition. After deposition, YBCO films were slowly cooled *in situ* in oxygen at a pressure of about 100 Torr.

The crystal structure of films was characterized using four-circle X-ray diffraction (XRD). The surface morphology of films was studied using optical microscopy and scanning electron microscopy (SEM). The composition of films was determined by Rutherford Backscattering Spectroscopy (RBS), which was performed at either AT&T Bell Labs or Charles Evans and Associates. Film thicknesses were measured using a Dektak profilometer. The room temperature resistivity of films was measured using a DC four-point probe. The critical temperature (T_C) of superconducting YBCO films was determined by DC four-point resistance versus temperature measurements or AC mutual inductance measurements. The critical current (J_C) of unpatterned YBCO films was determined by mutual inductance measurements. The microwave surface resistance of YBCO films was measured at 77 K and 96 GHz using a confocal resonator. The current-voltage characteristics of SNS junctions were studied using a curve tracer.

D. Technical Results

The building of the SSMOCVD system used for this contract was completed at Conductus during the beginning of the contract period. The system featured several design improvements based on joint work between Conductus and HP personnel at HP Labs, in which HP's SSMOCVD reactors were used. Further, the new reactor and substrate heater at Conductus were larger in size to easily accommodate substrates up to four inches in diameter.

The technical results will be presented in the following order: growth of YBCO, growth of $CaRuO_3$, growth of YBCO/$CaRuO_3$ bilayers, and fabrication of SNS junctions.

D.1 Growth of YBCO Films by SSMOCVD

Although the process developed at HP for the growth of high quality YBCO by SSMOCVD was transferred to Conductus, the changes in the reactor design resulted in the need to re-optimize the YBCO precursor powder composition and growth parameters. In brief, within the time frame of the contract, the YBCO film quality was not fully optimized, but was brought to a usable condition for the purposes of the contract. The YBCO film quality would be optimized for the Phase II contract.

YBCO films were grown on (100) $LaAlO_3$ substrates up to two inches in diameter. The YBCO films exhibited good electrical properties, with $T_C \cong 90$ K and $J_C > 1 \times 10^6$ A/cm^2 at 77 K. The microwave surface resistance (R_S) was typically < 1 mΩ at 77 K and 10 GHz, with a uniformity across two inch substrates of better than ± 15%. The best R_S was ≅ 0.5 mΩ at 77 K and 10 GHz, which compared favorably to the best R_S obtained at HP for SSMOCVD YBCO, which was 0.4 mΩ.

The YBCO films were epitaxial with the c-axis normal to the plane of the substrate, as illustrated by the XRD data in Figure 3, in which only (00ℓ) YBCO peaks are present. The FWHM of the (005) peak in θ-2θ scans was less than 0.25 degrees. Internally, we consider an (005) FWHM value less than 0.35 degrees to be adequate and a value of less than 0.30 degrees to indicate good epitaxy.

No a-axis oriented YBCO was evident in XRD χ scans. XRD φ scans showed that the films had excellent in-plane alignment of the a-b planes. The peak labeled as "?"

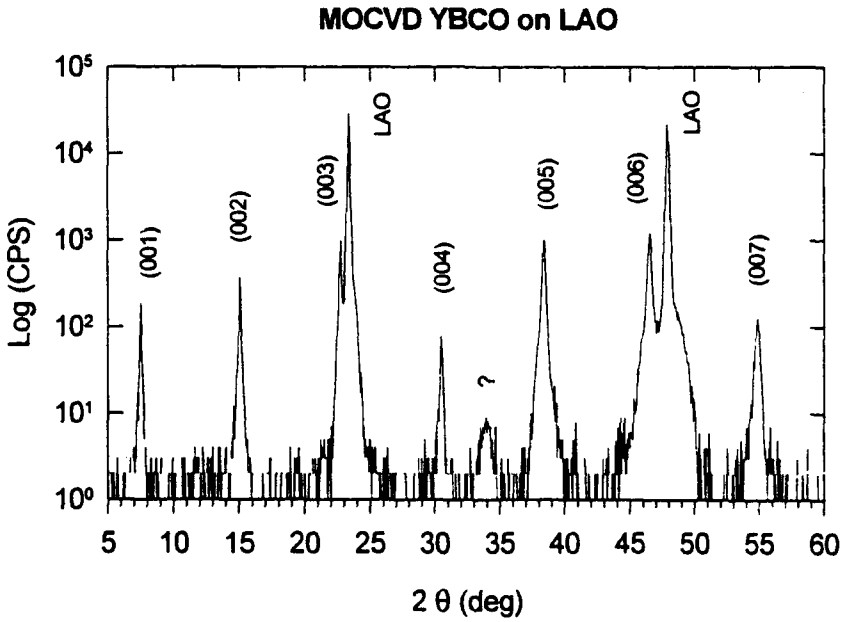

Figure 3. XRD data for YBCO film grown by SSMOCVD on (100) $LaAlO_3$.

in Figure 3 was usually present, but could not be clearly identified. It was most likely due to the presence of Y_2O_3, which has been found to grow as small, epitaxial inclusions within YBCO films grown by sputtering or laser ablation [7,8].

The surface morphology of YBCO films grown by SSMOCVD is shown in Figures 4a and 4b. Both films were grown under the same conditions, with substrate temperature = 780 °C, pressure = 0.83 Torr, and $P_{Ar}/P_{O2} \cong 1$. Only the precursor powder compositions were different. In Figure 4a, the background YBCO is smooth except for occasional pits. However, on the surface of the film are boulders which are about 0.5 μm in diameter and distributed at about 1 boulder every 2 μm^2. These boulders have been identified in other studies of YBCO films as polycrystalline CuO

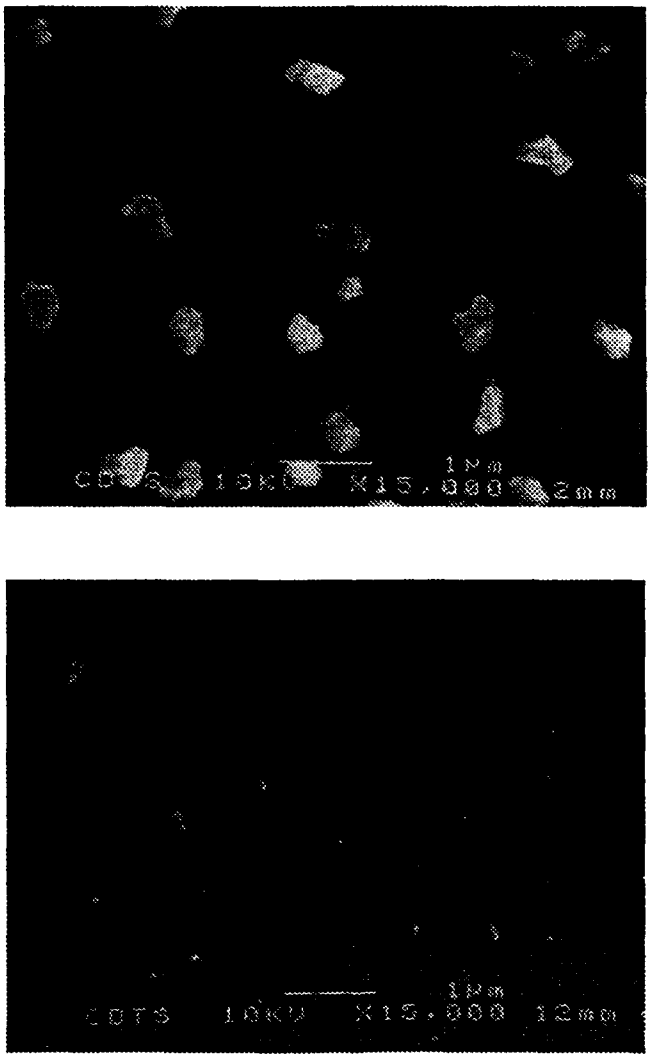

(a)

(b)

Figure 4. SEM micrographs of surface of YBCO films grown with precursor powder compositions, Y:Ba:Cu, of (a) 1.0:3.0:1.9 and (b) 1.0:1.9:2.8 (15 kX magnification).

[7,8]. Since the CuO is not structurally aligned with the YBCO or the $LaAlO_3$ substrate, CuO peaks do not appear in the θ-2θ XRD data in Figure 3.

The composition of the precursor powder used for the film shown in Figure 4a, expressed as the cation ratio Y:Ba:Cu, was 1.0:3.0:1.9. The composition of the film shown in Figure 4a, determined by RBS, was 1.0:1.7:3.1. Decreasing the Cu/Y ratio without changing the Ba/Y ratio in the precursor powder did not improve the film surface morphology significantly. However, increasing the Ba/Y ratio in the precursor powder, to a composition of 1.0:6.0:1.9, did decrease the size and area density of CuO boulders, as indicated in Figure 4b. The composition of the film shown in Figure 4b was 1.0:1.9:2.8. Thus changes in the films composition resulted in improvements in the surface morphology.

Ideally, a film composition of 1:2:3 should give a smooth YBCO surface, free of CuO boulders. This has been shown to be the case for YBCO films deposited by physical vapor deposition [9]. However, no groups have been able to controllably grow YBCO films by conventional MOCVD with surfaces free of CuO boulders. This is most likely due to the poor composition control of conventional MOCVD systems for YBCO, as discussed above in section A. The improvements in surface morphology in this work obtained by adjustments of the precursor powder composition suggest that with further refinements YBCO free of CuO boulders could be obtained. However, although the compositional control of SSMOCVD is superior to conventional MOCVD, there were still some inconsistency of the composition of YBCO films grown for this contract (± 5% for Cu/Y and ±15% for Ba/Y). The main reason for the inconsistency was thought to be the control of the vaporizer temperature in the SSMOCVD apparatus, which is presently being addressed and will be corrected before the Phase II contract. Regardless, the formation of CuO boulders on MOCVD YBCO films could be occurring via gas phase nucleation of CuO, in which case compositional control may not be the only factor. This issue needs further study.

A YBCO film surface should be as smooth as possible for the subsequent growth of additional epitaxial films on top of the YBCO film, as required for the SNS structure shown in Figure 1 . The presence of CuO boulders illustrated in Figure 4b on the YBCO surface would degrade the epitaxy of subsequent layers. However, it should be noted that although YBCO films grown by pulsed laser ablation have a rough surface morphology which includes large boulders, complicated multilayer structures have been successfully grown using laser ablation [1,10]. The difference between laser ablated and MOCVD YBCO films is that the boulders in laser ablated YBCO are usually epitaxial YBCO, over which subsequent layers can maintain epitaxy. This point illustrates that smooth, boulder-free films are not necessary for the growth of epitaxial multilayers.

D.2 Growth of $CaRuO_3$ Films by SSMOCVD

$CaRuO_3$ was chosen for use as the normal conductor in the SNS junction because it has an orthorhombic structure with a good pseudocubic lattice match to YBCO and has a suitable resistivity of ≅ 500 μΩ-cm at 300 K [1]. Prior to this contract, the growth

of $CaRuO_3$ by MOCVD had never been reported. A survey revealed that a suitable solid metalorganic Ru precursor was not available for the growth of $CaRuO_3$ by SSMOCVD. A Ca precursor, Ca-TMHD, was available. It was decided that Ru-TMHD would be the best solid Ru precursor, and Strem Chemical was paid to synthesize the Ru-TMHD. The synthesis was far more difficult than Strem Chemical estimated, resulting in a several week delay in getting the Ru-TMHD.

$CaRuO_3$ was grown by SSMOCVD on (100) $LaAlO_3$ and (100) $SrTiO_3$ substrates. $LaAlO_3$ was the substrate to be used in the SNS junction, as shown in Figure 1. $SrTiO_3$ was included because it provided better peak separation in XRD data from YBCO than did $LaAlO_3$, which was necessary to verify the epitaxy of the $CaRuO_3$. The substrate temperature for $CaRuO_3$ growth was 630 - 680 °C, which was 100 - 150 °C less than the value for YBCO. The Ca:Ru ratio in the precursor powder was 60:40 or 50:50. For the fabrication of the SNS structure shown in Figure 1, the $CaRuO_3$ film was only about 100 Å thick. For XRD measurements, $CaRuO_3$ films were grown 1000 Å thick to ensure adequate peak intensity.

$CaRuO_3$ films grown on (100) $SrTiO_3$ appeared dark gray in color and were conducting with a room temperature resistivity ≅ 600 - 800 μΩ-cm. $CaRuO_3$ films on (100) $LaAlO_3$ substrates had inconsistent appearance and electrical properties. Samples from the same run could appear either dark gray or nearly transparent, while the room temperature resistivity would be either ≅ 600 - 800 μΩ-cm or greater than 1 Ω–cm, respectively. A possible explanation for this inconsistency will be discussed below.

$CaRuO_3$ was found to grow epitaxially with a (110) orientation on (100) $SrTiO_3$, as illustrated in Figure 5. In this XRD analysis, the sample was tilted slightly off the normal to the $SrTiO_3$ substrate to suppress the substrate peaks. No other $CaRuO_3$ peaks

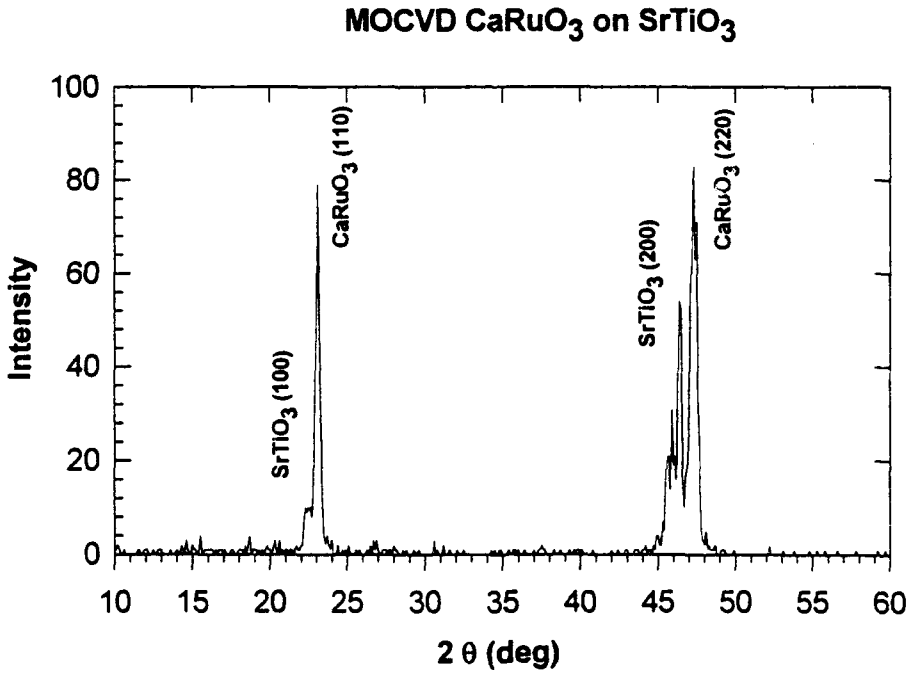

Figure 5. XRD data for $CaRuO_3$ grown by SSMOCVD on (100) SrTiO3.

were found, which was also true on $LaAlO_3$ substrates. The in-plane alignment of the $CaRuO_3$ films could not be verified due to overlap with $SrTiO_3$ or $LaAlO_3$ peaks.

The surface morphology of $CaRuO_3$ films depended strongly on the substrate temperature. A smooth surface morphology, as shown in Figure 6, was consistently obtained on $SrTiO_3$ substrates at a temperature of 680 °C. On $LaAlO_3$ substrates, the $CaRuO_3$ surface morphology was sometimes smooth but on electrically insulating samples the "wormy" morphology shown in Figure 7 was usually present. This wormy morphology suggested that the high resistivity of some $CaRuO_3$ films was due to incomplete wetting of the $LaAlO_3$ substrate. The reason for the incomplete wetting was not clear, but may have been due to the $LaAlO_3$ surface preparation.

The film stoichiometry may also have played a role in the film morphology and resistivity. Preliminary RBS composition measurements indicated that a Ca-Ru-O film on MgO was Ru deficient, with a Ca:Ru ratio of 1.0:0.5. RBS composition measurements on $LaAlO_3$ substrates were not possible due to peak overlap. Nonconducting Ca-Ru-O phases may have been present in addition to conducting $CaRuO_3$. However, no Ca-rich phases were found in XRD analysis to account for the excess Ca. Further, it was not certain if the sticking coefficients of Ca and Ru were the same on MgO as on $LaAlO_3$. The stoichiometry issue requires further study.

It is important to note that the inconsistency of the properties of $CaRuO_3$ films grown on $LaAlO_3$ was not only a problem for SSMOCVD. $CaRuO_3$ films grown in our laboratory by pulsed laser ablation also suffered from inconsistent electrical properties on $LaAlO_3$ substrates. A solution to the problem has recently been worked out for laser ablated $CaRuO_3$ which involves the deposition of a thin seed layer prior to $CaRuO_3$ growth. This would be applied to SSMOCVD growth of $CaRuO_3$ in a Phase II contract.

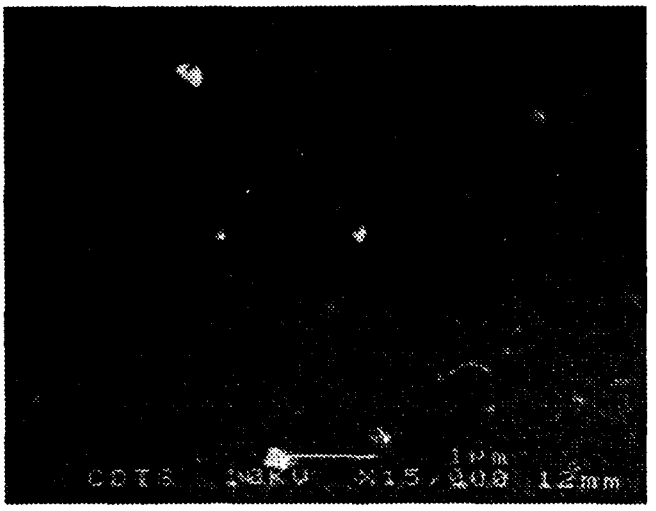

Figure 6. SEM micrograph of 1000 Å thick $CaRuO_3$ film on $SrTiO_3$ substrate (15 kX magnification).

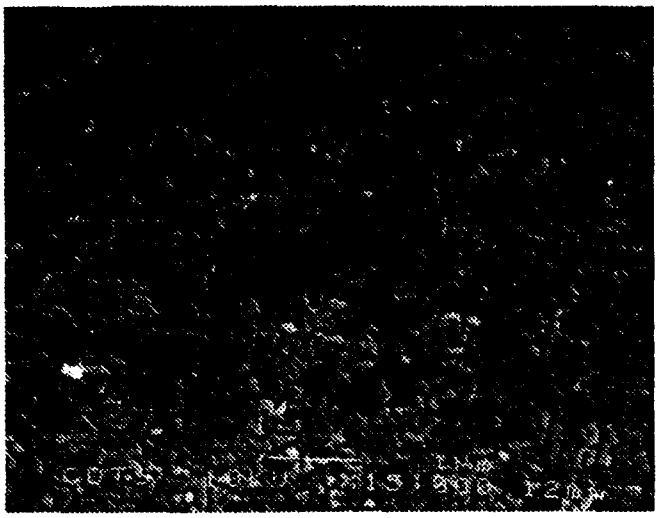

Figure 7. SEM micrograph of 1000 Å thick $CaRuO_3$ film on $LaAlO_3$ substrate (15 kX magnification).

D.3 Growth of $CaRuO_3$ / $YBa_2Cu_3O_{7-x}$ Bilayers by SSMOCVD

Bilayers of ≅ 100 Å $CaRuO_3$ followed by ≅ 2000 Å YBCO, as used in the SNS junction illustrated in Figure 1, were grown *in situ* by SSMOVCD on (100) $LaAlO_3$ substrates. The deposition parameters were chosen which gave the smoothest $CaRuO_3$ and YBCO film morphologies.

The T_C of the YBCO on top of $CaRuO_3$ was ≅ 85 K which was ≅ 5 K less than without a $CaRuO_3$ underlayer, but still acceptable for 77 K operation. The YBCO films were found by XRD to be epitaxial with a (00ℓ) orientation. No other YBCO peaks were evident. The FWHM value for the (005) peak in the θ-2θ scan was ≅ 0.32°, which was increased compared to YBCO alone but still respectable. No a-axis YBCO was evident in XRD χ scans and the in-plane alignment of the YBCO was found to be excellent in XRD ϕ scans. The surface morphology of the YBCO, under SEM examination, was similar to that of YBCO without the $CaRuO_3$ underlayer, as shown in Figure 4b.

D.4 Fabrication of SNS Edge Junction Using SSMOCVD

SNS edge junctions, as illustrated in Figure 1, were fabricated as follows. The base $SrTiO_3$/YBCO bilayer was grown on $LaAlO_3$ substrates by laser ablation. This was done for two reasons: 1) concern about the effect of the CuO boulders in the SSMOCVD YBCO on epitaxial overlayers and 2) a $SrTiO_3$ process had not been developed for SSMOCVD. Y_2O_3 or MgO, for which SSMOCVD processes had been developed, could have been used in place of $SrTiO_3$. However, the base $SrTiO_3$/YBCO bilayer needed to be grown *in situ*, and reason (1) was still a concern.

The laser ablated YBCO had $T_C \cong 89$ K and a (005) XRD FWHM of $\cong 0.25°$. The base $SrTiO_3$/YBCO bilayer was patterned by standard photolithography techniques and the sloped edge was formed by ion milling. The $CaRuO_3$/YBCO bilayer was then grown by SSMOCVD on top of the patterned $SrTiO_3$/YBCO base layers. An important issue during this step was effect of SSMOCVD processing on the properties of the base YBCO. The SSMOCVD $CaRuO_3$/YBCO bilayer was then patterned using standard photolithography techniques, including the provision that contacts could be made to both the base and top YBCO layers. Finally, gold contacts were deposited. The mask used to pattern the SNS junctions also included SQUIDs for testing of the SNS junctions in devices.

Before patterning, the top YBCO layer was found to have $T_C \cong 82$ K. The surface morphology of the top YBCO was slightly rougher than that shown in Figure 4b. Further, the top YBCO was epitaxial and (00ℓ) oriented with good in-plane alignment and no a-axis material present. The (005) FWHM in θ-2θ XRD data was $\cong 0.4°$, indicating that the epitaxial quality of the top YBCO was somewhat degraded. Regardless, these results were encouraging since they showed that even in an initial effort SSMOCVD could be successfully applied to the growth of YBCO multilayers. The quality of the multilayers would be certainly improved with further work.

Current versus voltage measurements were performed at temperatures down to 4 K on several junctions from different runs. The data from measurements at 77 K on one of the samples are presented in Figure 8, which did not match those of the desired resistively-shunted superconductive junction [1]. Rather, the junction had a high resistance on the order of 10 kΩ . This was true for this junction down to 4 K, and for the other junctions fabricated and tested. Since the junction was not superconducting, the SQUID device was not tested.

The reasons for the YBCO/$CaRuO_3$/YBCO junctions having high resistances were not clear. The SSMOCVD growth of the top $CaRuO_3$/YBCO bilayer did not degrade the bottom YBCO, since after stripping off the top $CaRuO_3$/YBCO layers, the T_C of the bottom YBCO was measured to still be 89 K. Another possibility was that the SSMOCVD $CaRuO_3$ and bottom YBCO reacted at the edge of the junction, which could have occurred if the Ca-Ru-O was off-stoichiometry. Physical characterization is needed to test this idea.

The most likely explanation for the high resistance of the junctions was that the $CaRuO_3$ layer was electrically insulating, as had been observed for the growth of $CaRuO_3$ on $LaAlO_3$. This does not necessarily imply that $CaRuO_3$ should be abandoned as the normal conducting layer for SSMOCVD growth of SNS junctions. As discussed above, although laser-ablated $CaRuO_3$ films have exhibited inconsistent electrical properties on $LaAlO_3$ substrates, a solution was developed which would be applied to the growth of $CaRuO_3$-based SNS junctions by SSMOCVD in a Phase II contract.

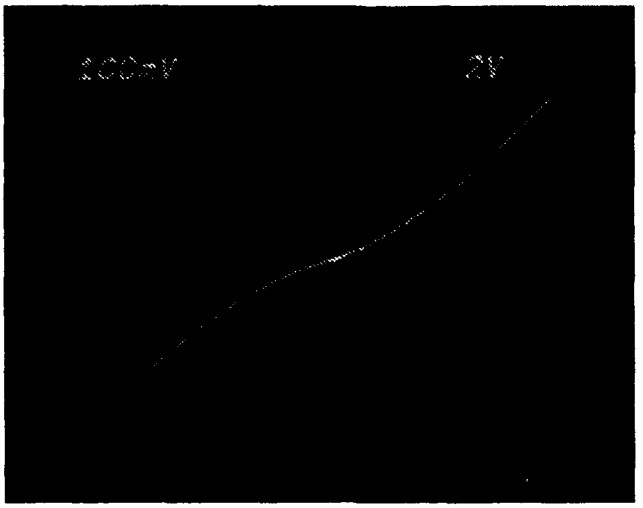

Figure 8. Current-voltage data at 77 K for YBCO/$CaRuO_3$/YBCO SNS junction made using SSMOCVD. Plot scales are 100 μA/division vertical and 2 V/division horizontal.

E. Important Findings and Conclusions

Conductus now has the capability for the growth of superconducting YBCO and other epitaxial oxides by SSMOCVD on substrates up to four inches in diameter, as required for the commercial scale production of HTS devices. SSMOCVD was applied in this contract to the growth of YBCO and $CaRuO_3$ films as required for SNS Josephson junctions.

A process was developed for the growth of epitaxial $CaRuO_3$ films by SSMOCVD, which was the first reported growth of $CaRuO_3$ by MOCVD. On $SrTiO_3$ substrates, $CaRuO_3$ films were consistently normal conductors with resistivities of 600 - 800 μΩ-cm. However, the room temperature resistivity of the $CaRuO_3$ films on $LaAlO_3$ substrates was either ≅ 600 - 800 μΩ-cm or greater than 1 Ω–cm. The problem of the inconsistent electrical properties of $CaRuO_3$ grown by SSMOCVD on $LaAlO_3$ substrates can be solved for the Phase II contract by using a thin seed layer prior to $CaRuO_3$ growth, as has been done for laser ablated $CaRuO_3$.

Second, a process was developed for the *in situ* growth of epitaxial YBCO/$CaRuO_3$ bilayers by SSMOCVD. The YBCO top layer had good electrical and physical properties. However, small CuO boulders were present on the YBCO surface which could present problems for the growth of subsequent epitaxial layers. The elimination of CuO boulders from the surface of YBCO films grown by SSMOCVD is primarily a composition control issue and is currently being addressed.

Finally, epitaxial SNS edge junctions were fabricated using a top YBCO/$CaRuO_3$ bilayer grown *in situ* by SSMOCVD and a base $SrTiO_3$/YBCO bilayer grown *in situ* by

pulsed laser ablation. The top and bottom YBCO layers were of good quality after the SSMOCVD layer growth. The junctions which were fabricated were found to be highly resistive. This was probably the result of a high resistivity for the $CaRuO_3$ layer, a problem which will be corrected for the Phase II contract.

F. Implications for Future Research

The results of this Phase I effort were encouraging since it was shown that SSMOCVD can be successfully applied to the growth of the materials and multilayers required for the fabrication of devices based on SNS edge junctions. The problems which were encountered could all be solved with a reasonable amount of effort before or during the Phase II contract.

Phase II of this program would be to extend the SSMOCVD process to the fabrication of SNS devices on four inch diameter substrates. This will be achieved by fabricating and testing a suitably complex Josephson integrated circuit using the SNS junctions developed under Phase I. This circuit might be a signal processing circuit such as shift register or analog-to-digital converter, or perhaps a sequence of gates based on a flux quantum logic family. Conductus is currently working on development of such HTS-based circuits on 1 cm x 1 cm substrates using films grown by laser ablation.

Due to the commercial importance of SNS junction technology to Conductus' commercial products, development of improved SNS junction fabrication procedures and N layer materials is being aggressively pursued. A Phase II contract would complement these efforts. Conductus is continuing to extend the capabilities in fabricating HTS-based circuits in its government-funded and internal programs so that we are confident that superconducting components of significant interest can be considered for this project.

G. Significant Hardware Development

No significant hardware development was funded by this contract.

References

1. K. Char, M.S. Colclough, T.H. Geballe, and K.E. Meyers, Appl. Phys. Lett. **62**, (1993).
2. K. Zhang, E.P. Boyd, B.S. Kwak, A.C. Wright, and A. Erbil, Appl. Phys. Lett. **55**, 1258, (1989).
3. L.M. Tonge, D.S. Richeson, T.J. Marks, J. Zhao, J.M. Zhang, B.W. Wessels, H.O. Marcy, and C.R. Kannewurf, Adv. Chem. Ser. **226**, 351 (1990).
4. R. Hiskes, S.A. DiCarolis, J.L. Young, S.S. Laderman, R.D. Jacowitz, and R.C. Taber, Appl. Phys. Lett. **59**, 606 (1991).
5. R. Hiskes, S.A. DiCarolis, R.D. Jacowitz, Z. Lu, R.S. Feigelson, and J.L. Young, Jour. Crystal Growth, **128**, 781 (1993) .
6. Z. Lu, R.S. Fiegelson, R.K. Route, S.A. DiCarolis, R. Hiskes, and R.D. Jacowitz, Jour. Crystal Growth, **128**, 920 (1993).
7. E. Olsson and K. Char, Appl. Phys. Lett. **64**, 1292 (1994).
8. E. Olssen, to be published.
9. R.G. Humphreys, N.G. Chew, J.S. Satchell, S.W. Goodyear, J.A. Edwards, and S.E. Blenkinsop, IEEE Trans. Mag. **27**, 1357 (1991).
10. L.P. Lee, K. Char, M.S. Colclough, and G. Zaharchuk, Appl. Phys. Lett. **59**, 3051 (1991).